Consensus via multi-population robust mean-field games

D. Bauso[a,b]

[a]*Department of Automatic Control and Systems Engineering, The University of Sheffield, Mappin Street, Sheffield, S1 3JD, United Kingdom*
[b]*Dipartimento di Ingegneria Chimica, Gestionale, Informatica, Meccanica, Università di Palermo, V.le delle Scienze, 90128 Palermo, Italy.*

Abstract

In less prescriptive environments where individuals are told 'what to do' but not 'how to do', synchronization can be a byproduct of strategic thinking, prediction, and local interactions. We prove this in the context of multi-population robust mean-field games. The model sheds light on a multi-scale phenomenon involving fast synchronization within the same population and slow inter-cluster oscillation between different populations.

Keywords: Synchronization, Consensus, Mean-field games

1. Introduction

Synchronization is a natural phenomenon which arises in many applications such as pricing in finance [2, 5], opinion dynamics [13], or transient stability of generators [3] etc. Most of the models for synchronization are derived in prescriptive environments in which individuals, the agents, are pre-programmed to adopt specific behaviors, see [12] and references therein.

In this paper we consider a multi-population of dynamic agents as illustrated in Fig. 1.

The dynamics of each agent — henceforth referred to as *microscopic* dynamics — describes the time evolution of its state in the form of a stochastic differential equation. In addition, for each population of agents, we consider the corresponding *phase coherence*, which is a measure of the synchronization of the agents of that population, and the associated dynamics, the latter called *macroscopic* dynamics. Each agent seeks to synchronize its phase to

Email address: d.bauso@sheffield.ac.uk (D. Bauso)

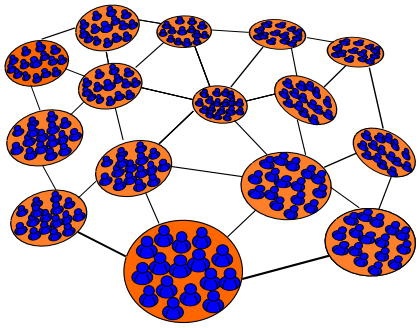

Figure 1: Multi-population model with local interactions.

the local average phase obtained via mean-field computation. The model highlights the following aspects: i) each agent is a rational player equipped with strategic and computation capabilities; ii) the interaction is local and subject to disturbances; iii) agents are heterogeneous. Local interaction is determined by geographic proximity between two populations, and is modeled by a network topology where the nodes are the populations and the links establish neighbor relations. The model is a multi-population robust mean-field games within the theory proposed by M.Y. Huang, P. E. Caines and R. Malhamé in [6, 7, 8] and independently by Lasry and Lions in [10]. For a survey see [4]. Modeling synchronization as a game is also in [15]. Game theoretic learning is also discussed in [16]. Efficiency loss in equilibria is studied in [17]. Higher level interactions between the subpopulations are analyzed in [9] in the context of auctions. While sharing some of the general concepts already present in the aforementioned references, this paper adds new elements such as local interactions, disturbances and heterogeneity in a unified framework.

Main contribution. This paper shows that synchronization can be obtained in less prescriptive environments as byproduct of strategic thinking, prediction, and local interactions, see Fig. 2. Even if the agents are not pre-programmed to adopt certain strategies, a proper mix of the above three factors will lead to synchronization. To address model misspecification, the game involves the presence of an adversarial disturbance which captures uncertainty in the microscopic dynamics (i.e. some players may be irrational). The resulting game is then a robust mean-field game as the one in [1] and in the same spirit as [14].

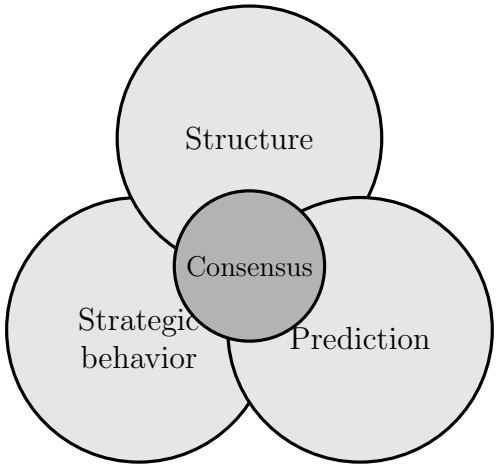

Figure 2: Synchronization as a result of a proper mix of strategic thinking, prediction, and local interaction in a structured environment.

The model involves a system of coupled partial differential equations (PDEs). For each population we have one PDE in the form of a Hamilton-Jacobi-Isaacs (HJI) equation, and a second PDE which is the Fokker-Planck-Kolmogorov (FPK) equation describing the diffusion process of the agents' states. We provide a solution of the HJI equation under the assumption that the time evolution of the common state is given. We show that the problem reduces to solving three matrix equations and that in the infinite horizon case the macroscopic dynamics is a typical consensus dynamics.

The analysis of the mean-field game is then extended to the case of second-order dynamics. Even for this case, we prove that the problem of approximating mean-field equilibrium strategies reduces to solving three matrix equations. By taking the limit for $T \to \infty$ the macroscopic dynamics takes the form of a second-order consensus dynamics. Simulations of simple heuristics show the multi-scale nature of the process involving fast synchronization within the same population and slow inter-cluster oscillation capturing delays due to the geographic sparsity of the populations.

The remainder of the paper is structured as follows. In Section 2 we formulate the problem. In Section 3 we discuss examples. The main results are presented in Sections 4 and 5. Section 6 provides a numerical example. Finally in Section 7 we provide conclusions.

2. Model and problem set-up

Consider p populations of homogeneous agents (players); each player belongs to a population $k \in \{1, \dots, p\}$ and is characterized by a state $X(t) \in \mathbb{R}$ at time $t \in [0, T]$, where $[0, T]$ is the time horizon window. The control variable is a measurable function of time, $u(\cdot) \in U$, where U is the control set, defined as $t \mapsto \mathbb{R}$ and establishes the rate of variation of an agent's state. A disturbance tries to affect the agents' state in a way that is proportional to his efforts $w(\cdot) \in W$, where W is the control set of the disturbance.

The state dynamics of each player is

$$dX(t) = (u(t) + w(t))dt + \sigma d\mathcal{B}(t),\ t > 0, \tag{1}$$

where $X(0) = x$ for given initial state x, $\sigma > 0$ is a weighting coefficient and $\mathcal{B}(t)$ is the standard Brownian motion process.

For every population $k \in \{1, \dots, p\}$, consider a probability density function $m_k : \mathbb{R} \times [0, +\infty[\to \mathbb{R}$, $(x, t) \mapsto m_k(x, t)$, representing the density of agents of that population in state x at time t, which satisfies $\int_{\mathbb{R}} m_k(x, t)dx = 1$ for every t. Let the *mean state* of population k at time t be $\overline{m}_k(t) := \int_{\mathbb{R}} x m_k(x, t)dx$. From averaging both sides of (1) we get the aggregated dynamics

$$\frac{d}{dt}\overline{m}_k(t) = \overline{u}_k(t) + \overline{w}_k(t),$$

where $\overline{u}_k(t)$ and $\overline{w}_k(t)$ are the mean state-feedback control and disturbance of that population, i.e.,

$$\overline{u}_k(t) := \int_{\mathbb{R}} u(x, t)m_k(x, t)dx, \qquad \overline{w}_k(t) := \int_{\mathbb{R}} w(x, t)m_k(x, t)dx.$$

Let a graph $G = (V, E)$ be given where $V = \{1, \dots, p\}$ is the set of vertices, one per each population, and $E = V \times V$ is the set of edges. Although most results are easily generalizable to more general graphs, possibly time-varying, for the sake of simplicity we henceforth assume that $G = (V, E)$ is a connected undirected graph, see e.g. [12, Lemma 1]. Denote the set of neighbors of k by $N(k) = \{j \in V |\, (k, j) \in E\}$.

The objective of an agent is to adjust his state based on the aggregate kth state. Set

$$\rho_k = \frac{\sum_{j \in N(k)} \overline{m}_j(t)}{|N(k)|}, \tag{2}$$

where $|N(k)|$ denotes the cardinality of the set $N(k)$, namely the number of neighbors of k.

Then, for the agents, consider a running cost $g : \mathbb{R} \times \mathbb{R} \times U \to [0, +\infty[$, and a terminal cost $\Psi : \mathbb{R} \times \mathbb{R} \to [0, +\infty[$, given by:

$$g(x, \rho_k, u) = \frac{1}{2}\left[a(\rho_k - x)^2 + cu^2\right], \tag{3}$$

$$\Psi(\rho_k, x) = \frac{1}{2}S(\rho_k - x)^2. \tag{4}$$

The problem in abstract terms is then formulated as follows.

Problem 1. *Let $\mathcal{B}$ be a one-dimensional Brownian motion defined on the probability space $(\Omega, \mathcal{F}, \mathbb{P})$, where Ω is the set of outcomes of a random experiment, $\mathcal{F}$ is the natural filtration generated by $\mathcal{B}$, and $\mathbb{P}$ is a probability measure. Let the initial state $X(0)$ be independent of $\mathcal{B}$ and with density m_{k0}. Given a finite horizon $T > 0$, an initial distribution of the states $\overline{m}_{k0} : \mathbb{R} \to \mathbb{R}$, a running cost: $g : \mathbb{R} \times \mathbb{R} \times U \to [0, +\infty[$ as in (3); a terminal cost $\Psi : \mathbb{R} \times \mathbb{R} \to [0, +\infty[$ as in (4), and dynamics as in (1), solve*

$$\min_{u(\cdot)} \max_{w(\cdot)} \mathbb{E} \int_0^T \left[g(X(t), \rho_k(t), u(t)) - \tfrac{\gamma^2}{2} w(t)^2\right] dt + \Psi(\rho_k(T), X(T)),$$

where $\gamma > 0$, and $\mathcal{U}$, $\mathcal{W}$ are the sets of all measurable functions $u(\cdot)$ and $w(\cdot)$ from $[0, +\infty[$ to U, W respectively.

3. Examples

We review three examples of synchronization phenomena from different application domains. All examples are based on the model of Kuramoto networked-coupled oscillators [12]. Consider the synchronization of the phase angles of a set of N coupled oscillators, for which the dynamics of the ith oscillator is given by

$$\dot{\Theta}_i = \Omega_i + \frac{\mathcal{K}}{n} \sum_{j \in N} \sin(\Theta_j - \Theta_i),$$

where Θ_i is its phase and Ω_i is its (time-invariant) natural frequency. The coupling term on the RHS is responsible of synchronization in that regulates the angular velocity $\dot{\Theta}_i$ based on the deviation of the ith phase from the

average phase computed over the population. The level of synchronization increases with the parameter $\mathcal{K}$ present in the global coupling term.

The level of synchronization is captured by the complex order parameter

$$z = re^{i\Phi} = \frac{1}{n}\sum_{j=1}^{n} e^{i\Theta_i}, \tag{5}$$

where r is referred to as *phase-coherence* and Φ is the *average phase*.

Considering indistinguishable players and the corresponding asymptotic limit for $n \to \infty$ (we drop the index i) we have

$$\dot{\Theta}(t) = \omega + \mathcal{K} r \sin(\Phi(t) - \Theta(t)) \tag{6}$$

that, after linearization around zero, can be approximated by

$$\underbrace{\dot{\Theta}}_{\dot{X}(t)} = \underbrace{\omega}_{w(t)} + \underbrace{r(\Phi(t) - \Theta(t))}_{u(t)}. \tag{7}$$

Equation (7) is the deterministic version of (1) provided that $u(t) = r(\Phi(t) - \Theta(t))$ and $w(t) = \omega$. Through game-theoretic approach we wish to design $u(t)$ to incentivize synchronization among the oscillators. To do this, introduce a running cost and terminal penalty:

$$g(\delta, \Phi, u) = \tfrac{1}{2}\left[a(\Phi - \Theta)^2 + cu^2\right], \quad \Psi(\Phi, \delta) = \tfrac{1}{2} S(\Phi - \Theta)^2,$$

which are of the same types as (3) and (4), where ρ_k is replaced by Φ. It remains to show that the control $u(t) = r(\Phi(t) - \Theta(t))$ and the disturbance $w(t) = \omega$ can be obtained solving the min-max problem

$$\min_{u(\cdot)} \max_{w(\cdot)} \mathbb{E} \int_0^T \left[g(\delta(t), \Phi(t), u(t)) - \tfrac{\gamma^2}{2} w(t)^2 \right] dt + \Psi(\Phi(T), \delta(T)), \tag{8}$$

subject to the dynamics

$$d\delta(t) = \Big(\omega + r \sin(\Phi(t) - \delta(t))\Big) dt + \sigma d\mathcal{B}(t), \ t > 0.$$

Now consider p population of oscillators, at different geographic locations, with average angles interconnected via a network topology. Each population $k \in \{1, 2, \ldots, p\}$ represents a population of oscillators, and is characterized by an average phase Φ_k (the average phase is now indexed by the population

type). A network topology is used to model the interconnection between the average phases of two distinct populations of oscillators. The synchronization angle ρ_k for the population k is then expressed by the averaging law:

$$\rho_k = \frac{\sum_{j \in N(k)} \Phi_j(t)}{|N(k)|},$$

which is of the same form of (2) with $\overline{m}_j(t)$ replaced by $\Phi_j(t)$.

Example 1 (Stock price synchronization). *In the financial market, synchronization of stock prices arises during financial crisis (e.g. the Black Monday and the the global economic crisis of 2008) [2] or as a consequence of high speed trading [5]. Nodes correspond to stocks and the connections between two nodes are established according to a measurement related to the correlation between the temporal price evolutions of the respective stocks. The phase coherence increases, indicating the emergence of a collective behavior of stock prices, since most of them tend to have a similar evolution.*

Example 2 (Opinion dynamics). *The analogy assimilates oscillators to individuals, phases to opinions, and natural frequencies to natural opinion changing rates [13]. Global coupling is a result of the interactions among the individual, these depending on the respective distance between them. In this new perspective, the dynamic model (7) appears as a consensus dynamics (opinion synchronization), in which the coupling term accounts for "emulation" (an individual's opinion is influenced by those of its neighbours), and which includes an additional input representing the "natural changing rate".*

Example 3 (Transient stability of power grids). *It is well-known (see, e.g., [3]) that in a multi-machine power grid involving n generators, the rotor angle dynamics are interconnected and each rotor angle evolves according to the* swing equation *which resemble the classical* Kuramoto *oscillators' dynamics. The level of synchronization is the complex order parameter in (5) which is now called* common power angle*. Imagine multiple smart grids $k \in \{1, 2, \ldots, p\}$ each involving a population of generators. Populations are geographically sparse and the synchronization occurs locally by involving only neighbor populations. The average phase is now called common power angle Φ_k and is indexed by the population type. A network topology can be used to model the interconnection between the common power angles of the different populations of generators based on their relative geographic distance.*

4. The mean-field game formulation

For every population $k \in \{1, 2, \ldots, p\}$, denote by $v_k(x,t)$ the (upper) value of the robust optimization problem under worst-case disturbance starting at time t and at state x. The problem results in the following multi-population mean-field game in $v_k(x,t)$, and $m_k(x,t)$ for all $k \in \{1, 2, \ldots, p\}$:

$$\begin{array}{l} \partial_t v_k(x,t) + \{f(x,u_k^*,w_k^*)\partial_x v_k(x,t) + g(x,\rho_k(t),u_k^*) \\ -\frac{\gamma^2}{2}w_k^*(t)^2\Big\} + \frac{\sigma^2}{2}\partial_{xx}^2 v_k(x,t) = 0, \quad \text{in } \mathbb{R}\times[0,T[, \\ v_k(x,T) = \Psi_k(\rho_k(T),x) \text{ in } \mathbb{R}, \\ \partial_t m_k(x,t) + div(m_k(x,t)f(.)) - \dfrac{\sigma^2}{2}\partial_{xx}^2 m_k(x,t) = 0\,, \text{in } \mathbb{R}\times[0,T[, \\ m_k(x,0) = m_{k0}(x) \text{ in } \mathbb{R}, \end{array} \tag{9}$$

where the aggregate variables are given by

$$\overline{m}_k(t) := \textstyle\int_{\mathbb{R}} x m_k(x,t)dx, \quad \rho_k = \dfrac{\sum_{j\in N(k)}\overline{m}_j(t)}{|N(k)|}, \tag{10}$$

and where u_k^* and w_k^* are the optimal time-varying state-feedback control and disturbance for every single agent in population k obtained as

$$\begin{array}{l} u_k^*(x,t) \in \text{argmin}_{u\in\mathcal{U}}\{f(x,u,w_k^*)\partial_x v_k(x,t) + g(x,\rho_k(t),u)\}, \\ w_k^*(x,u_k^*,t) \in \text{argmax}_{w\in\mathcal{W}}\{f(x,u_k^*,w)\partial_x v_k(x,t) + g(x,\rho_k,u_k^*) - \frac{\gamma^2}{2}w^2\}. \end{array} \tag{11}$$

Note that the function $f(x,u,w)\partial_x v_k(x,t) + g(x,\rho_k,u) - \frac{\gamma^2}{2}w^2$ is strictly concave in w and strictly convex in u for $\gamma > 0$ and $c > 0$, and hence there exists a saddle point (u_k^*, w_k^*). Any solution of the above system of equations is referred to as *worst-disturbance feedback mean-field equilibrium.*

Let the Hamiltonian (without disturbance w) be given by $H(x,\tilde{p},\rho_k) = \inf_u\{g(x,\rho_k,u) + \tilde{p}u\}$, where $\tilde{p}$ is the co-state. The robust Hamiltonian is

$$\tilde{H}(x,\tilde{p},\rho_k) = H(x,\tilde{p},\rho_k) + \sup_w\left\{\tilde{p}w - \frac{1}{2}\gamma^2 w^2\right\}.$$

After solving for w we obtain $w_k^* = \frac{1}{\gamma^2}\partial_x v_k(x,t)$. Introducing the Hamiltonian

and the expression for w_k^* in the mean-field system (9) we obtain

$$\begin{array}{l}
\partial_t v_k(x,t) + H(x,\tilde{p},\rho_k) + \dfrac{1}{2\gamma^2}(\partial_x v_k(x,t))^2 + \dfrac{\sigma^2}{2}\partial^2_{xx} v_k(x,t) = 0, \text{ in } \mathbb{R}\times[0,T[,\\
v_k(x,T) = \Psi(\rho_k(T),x) \text{ in } \mathbb{R},\\
\partial_t m_k(x,t) + \partial_x\Big(m_k(x,t)\partial_{\tilde{p}} H(x,\tilde{p},\rho_k)\Big)\\
+\frac{1}{\gamma^2}\partial_x\Big(m_k(x,t)\partial_x v_k(x,t)\Big) - \frac{\sigma^2}{2}\partial^2_{xx} m_k(x,t) = 0, \quad \text{in } \mathbb{R}\times[0,T[,\\
m_k(x,0) = m_{k0}(x) \text{ in } \mathbb{R},\\
\overline{m}_k(t) := \int_{\mathbb{R}} x m_k(x,t)dx, \quad \rho_k = \frac{\sum_{j\in N(k)}\overline{m}_j(t)}{|N(k)|}.
\end{array} \tag{12}$$

We are now ready to specialize the results obtained above to the case of a multi-population with affine dynamics as in Problem 1.

Theorem 1. *Problem 1 admits the robust mean-field game reformulation*

$$\begin{array}{l}
\partial_t v_k(x,t) + \Big(-\frac{1}{2c} + \frac{1}{2\gamma^2}\Big)|\partial_x v_k(x,t)|^2\\
+\frac{1}{2}a(\rho_k(t)-x)^2 + \frac{1}{2}\sigma^2\partial^2_{xx} v_k(x,t) = 0, \ \textit{in } \mathbb{R}\times[0,T[,\\
v_k(x,T) = \Psi(\rho_k(T),x), \ \textit{in } \mathbb{R},\\
\partial_t m_k(x,t) + \Big(\frac{1}{2\gamma^2} - \frac{1}{2c}\Big)\partial_x\Big(m_k\partial_x v_k\Big) - \frac{1}{2}\sigma^2\partial^2_{xx} m_k(x,t) = 0,\\
m_k(x,0) = m_{k0}(x) \ \textit{in } \mathbb{R},\\
\overline{m}_k(t) := \int_{\mathbb{R}} x m_k(x,t)dx, \quad \rho_k = \frac{\sum_{j\in N(k)}\overline{m}_j(t)}{|N(k)|}.
\end{array} \tag{13}$$

Furthermore, the optimal control and worst-case disturbance are

$$u_k^*(x,t) = -\frac{1}{c}\partial_x v_k(x,t), \qquad w_k^*(x,t) = \frac{1}{\gamma^2}\partial_x v_k(x,t). \tag{14}$$

The significance of the above result is that to find the optimal control input we need to solve the two coupled PDEs in (13) in v and m with given boundary conditions (the second and fourth conditions).

Remark 1. *Sufficient conditions for the existence of a classical solution for (13)-(14) are discussed in Theorem 2.6 in [10] and also in Theorem 1 and 2 in [4]. Such conditions are based on the following assumptions, which are verified in our problem formulation. The initial measure $m_{k0}(.)$ is absolutely continuous with a continuous density function with finite second moment, and the terminal penalty $\Psi(.)$ is smooth, bounded and Lipschitz continuous. In addition, the running cost $g(.)$ is convex in $u_k(.)$ and concave in the disturbance $w_k(.)$. The drift is linear and hence Lipschitz continuous.*

5. Mean-field equilibrium

This section investigates the solution of the HJI equation under the assumption that the time evolution of the common state is given. We show that the problem reduces to solving three matrix equations. In the limit case in which $T \to \infty$ the macroscopic dynamics is a typical consenus dynamics.

Given $\rho_k(t)$, for $t \in [0,T]$, consider the problem

$$\begin{array}{c} \min\limits_{u(\cdot)} \max\limits_{w(\cdot)} \mathbb{E} \displaystyle\int_0^T \Big[g(X(t), \rho_k(t), u(t)) - \frac{\gamma^2}{2} w(t)^2 \Big] dt \\ \text{subject to} \quad dX(t) = (u(t) + w(t))dt + \sigma d\mathcal{B}(t), \ t > 0. \end{array} \tag{15}$$

The next result provides mean-field equilibrium control and disturbances.

Theorem 2. ***(Worst-case mean-field equilibrium)*** *A mean-field equilibrium for (13) is as follows: For all $k \in \{1, 2, \ldots, p\}$*

$$\begin{array}{l} v_k(x,t) = \frac{1}{2}\phi(t)x^2 + h(t)x + \chi(t), \\ \dot{\overline{m}}_k(t) = (-\frac{1}{c_1} + \frac{1}{\gamma^2})(\phi(t)\overline{m}_k(t) + h(t)), \end{array} \tag{16}$$

where

$$\begin{array}{l} \dot{\phi}(t) + \left(-\frac{1}{c_1} + \frac{1}{\gamma^2}\right)\phi(t)^2 + a = 0 \ \textit{in} \ [0,T[, \ \phi(T) = S, \\ \dot{h}(t) + \left(-\frac{1}{c_1} + \frac{1}{\gamma^2}\right)\phi(t)h(t) - a\rho_k(t) = 0 \ \textit{in} \ [0,T[, \ h(T) = -S\rho_k(T), \\ \dot{\chi}(t) + \left(-\frac{1}{2c_1} + \frac{1}{2\gamma^2}\right)h(t)^2 + \frac{1}{2}a\rho_k(t)^2 + \frac{1}{2}\sigma^2\phi(t) = 0 \\ \textit{in} \ [0,T[, \ \chi(T) = \frac{1}{2}S\rho_k^2(T). \end{array} \tag{17}$$

The corresponding mean-field equilibrium control and disturbance are

$$u^*(X,t) = -\frac{1}{c_1}(\phi(t)X + h(t)), \qquad w^*(X,t) = \frac{1}{\gamma^2}(\phi(t)X + h(t)). \tag{18}$$

Furthermore, for $T \to \infty$, set $\overline{m} = (\overline{m}_1, \overline{m}_2, \ldots, \overline{m}_p)^T$. Then

$$\dot{\overline{m}}(t) = -L\overline{m}(t), \tag{19}$$

where $L = [L_{kj}]$ is the graph-Laplacian defined as follows:

$$L_{kj} = \begin{cases} \phi(\frac{1}{c_1} - \frac{1}{\gamma^2}) & j = k, \\ -\phi(\frac{1}{c_1} - \frac{1}{\gamma^2})\frac{1}{|N(k)|} & j \in N(k), \ j \neq k, \\ 0 & \textit{otherwise.} \end{cases} \tag{20}$$

The relevance of the above result is that (17) can be solved in closed form. We henceforth refer to $\overline{m}$ as the vector of *aggregate states*.

Remark 2. *Theorem 2 synthesizes the claim that synchronization can be obtained as a byproduct of strategic thinking, prediction and local interactions. Actually, dynamics (19) is a consensus dynamics and as such it guarantees synchronization. Dynamics (19) is a direct consequence of (18) and it is not obtained by pre-programming the agents to adopt a specific behavior. Furthermore, the control and disturbance in (18) are based on $\phi(t)$ and $h(t)$ obtained from the final value problem (17). This requires* prediction *on future values of $\phi(t)$ and $h(t)$. By* Local interaction *we refer to the use of neighbor relations in (20) to calculate $\overline{m}_k(t)$ for the kth population.* □

The next result investigates the speed of convergence of dynamics (19) and uses and adapt some results from [12]. Let $\lambda_2(\phi)$ be the second smallest eigenvalue of the graph-Laplacian matrix L. We write $\lambda_2(\phi)$ to stress the dependency of the eigenvalue on the solution ϕ of the differential Riccati equation (17) and the corresponding algebraic Riccati equation obtained from it by considering the stationary case. Introduce now the disagreement vector

$$\xi = \overline{m} - \eta \mathbf{1}, \tag{21}$$

for any $\eta \in \mathbb{R}$ and where $\mathbf{1}$ is a vector of 1s, and the disagreement function

$$\nu(\xi) = \xi^T \xi. \tag{22}$$

Corollary 1. ***(Performance of synchronization)*** *Let $\lambda_2(\phi)$ be the second smallest eigenvalue of the Laplacian L and let a disagreement function $\nu(\xi)$ be defined as in (21)-(22). Then the disagreement function satisfies*

$$\dot{\nu}(\xi(t)) \leq -2\lambda_2(\phi)\nu(t). \tag{23}$$

The above result states that consensus is reached exponentially fast and with a speed which is lower bounded by the second smallest eigenvalue $\lambda_2(\phi)$.

Note that by substituting the mean-field equilibrium strategies $u^* = -\frac{1}{c_1}(\phi(t)X + h(t))$ and $w^* = \frac{1}{\gamma^2}(\phi(t)X + h(t))$ as given in (18) in the open-loop microscopic dynamics $dX(t) = (u(t) + w(t))dt + \sigma d\mathcal{B}(t)$ as defined in (15), the closed-loop microscopic dynamics is

$$dX(t) = \left(-\tfrac{1}{c_1} + \tfrac{1}{\gamma^2}\right)\Big(\phi(t)X(t) + h(t)\Big)dt + \sigma d\mathcal{B}(t),\ t > 0. \tag{24}$$

set/parameters	n	x_{min}	x_{max}	dt	$std(m_0)$	T	$\overline{m}_0$	σ	θ	$\tilde{\theta}$	$\hat{\theta}$
1st set	10^3	-50	50	1	15	30	0	1	0.3	0.25	0.9
2nd set	10^3	-50	50	1	15	50	0	1	0.5	$0.1, 0.35, 0.55$	0.9
3rd set	10^3	-50	50	1	15	50	0	1,5,9	0.5	0.25	0.9

Table 1: Simulation parameters.

Let $V(X(t)) = dist(X(t), \mathcal{X})$, where $dist(X(t), \mathcal{X})$ denotes the Euclidean distance of $X(t)$ from the set $\mathcal{X}$. The next result establishes a condition under which the above dynamics converges asymptotically to the set of equilibrium points in a stochastic sense [11].

Corollary 2. ***(2nd-moment stability)*** *Let a compact set $\mathcal{M} \subset \mathbb{R}^2$ be given. Suppose that for all $X \notin \mathcal{M}$*

$$\partial_X V(X,t)^T \left(-\tfrac{1}{c_1} + \tfrac{1}{\gamma^2}\right) \Big(\phi(t)X(t) + h(t)\Big) < -\tfrac{1}{2}\sigma^2 \partial_{xx} V(X,t). \tag{25}$$

Then the dynamics (24) is a stochastic process with 2nd moment bounded.

6. Simulation example

The parameters of the simulation studies are summarized in Table 1. The numerical studies have been conducted considering a thousand of players, five populations, and a discretized set of states $\mathcal{X}$ from $x_{min} = -50$ to $x_{max} = 50$. Graph G is a chain, see Fig. 3. The step size is $dt = 1$ and the horizon is $T = 30$ in the first set of simulations and $T = 50$ in the other two sets.

The evolution of the state of each single player is

$$X(t+1) = X(t) + \hat{\xi}(\rho_k - X) + \sigma\, rand[-1, 1]. \tag{26}$$

Note that the above is a discretized version of (24). The initial state x is randomly extracted as explained in the following. Also we consider a discretized version of the second-order consensus dynamics by setting

$$\overline{m} = (\overline{m}_1, \ldots, \overline{m}_5, \dot{\overline{m}}_1, \ldots, \dot{\overline{m}}_5)^T.$$

We assume that the control and disturbance enter in the right-hand-side of a second-order linear differential equation. Using the compact notation

$$\mu_{\bullet 1}(t) = \left(\ \overline{m}_1(t), \ldots, \overline{m}_5(t) \ \right)^T, \quad \mu_{\bullet 2}(t) = \left(\ \dot{\overline{m}}_1(t), \ldots, \dot{\overline{m}}_5(t) \ \right)^T,$$

the dynamics has the form of the second-order consensus dynamics:

$$\begin{bmatrix} \mu_{\bullet 1}(t) \\ \mu_{\bullet 2}(t) \end{bmatrix} = \begin{bmatrix} I & I \\ -\theta L & -\tilde{\theta}(L + \hat{\theta} I) + I \end{bmatrix} \begin{bmatrix} \mu_{\bullet 1}(t-1) \\ \mu_{\bullet 2}(t-1) \end{bmatrix} \ t = 1, 2, \ldots, T; \tag{27}$$

$$\mu_{\bullet 1}(0) = (\overline{m}_1(0), \ldots, \overline{m}_5(0))^T, \quad \mu_{\bullet 2}(t) = (\dot{\overline{m}}_1(t), \ldots, \dot{\overline{m}}_5(t))^T = (0, \ldots, 0)^T,$$

and where L is the normalized (one for the entries on the main diagonal, and the reciprocal of the degree of node i for each adjacent node of i in the ith row) Laplacian matrix of the communication graph $G = (N, E)$. The elastic and damping coefficients θ, $\hat{\theta}$ and $\tilde{\theta}$ are as in Table 1.

We assume m_0 to be Gaussian with mean $\overline{m}_0$ equal to 0. The standard deviation $std(m_0)$ is set to 15. Then, the initial state x in (26) is obtained from a random realization with density distribution law m_0.

Figure 4 shows the time history of the microscopic evolution of each agent's state. Two phenomena can be observed at two different time-scale. First, on a fast time-scale, agents in each single population $k \in \{1, \ldots, 5\}$ synchronize to the local aggregate state ρ_k. Second, on a slower time-scale, local aggregate states synchronize via second-order consensus dynamics. This explains the inter-cluster oscillations clearly shown in the time plot.

In a second set of simulations we investigate the role of the elastic and damping coefficients θ, $\hat{\theta}$ and $\tilde{\theta}$. In particular, we simulate three different scenarios corresponding to an increasing damping coefficient $\tilde{\theta} = 0.1, 0.35, 0.55$. To investigate how the system responds to periodic impulsive perturbations, we reset the state to the initial value every 10 time units. The resulting time plot is displayed in Fig. 5. On the left column we have the time plot of the microscopic dynamics while on the right column we have the time plot of the standard deviation. The damping effect is visually clear from top to bottom in the plots of the left column.

A third set of simulations highlights the effects of the Brownian motion. Here we consider three scenarios associated to three different values of the parameter $\sigma = 1, 2, 3$. The resulting time plot is displayed in Fig. 6, where we have the time plot of the microscopic dynamics on the left column and the time plot of the standard deviation on the right column. As in the previous

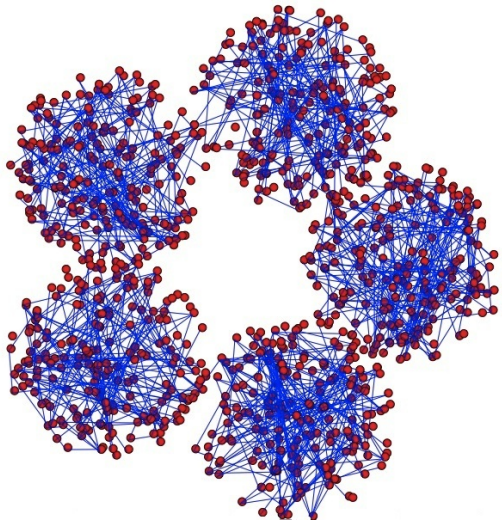

Figure 3: A thousand of players split into five populations with chain interaction topology.

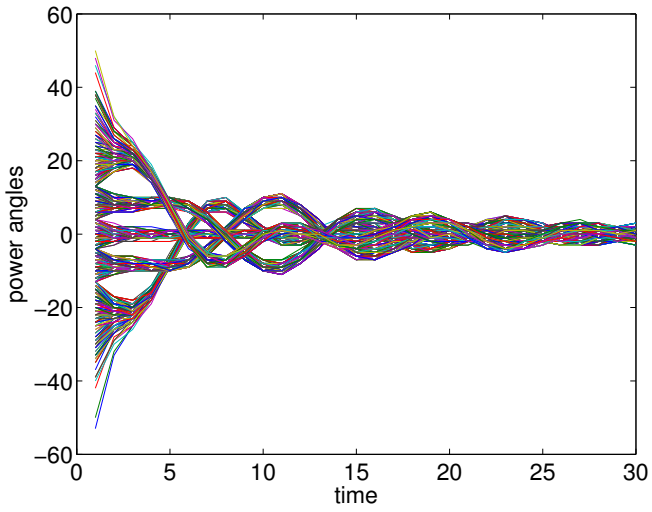

Figure 4: Inter-cluster oscillations due to local interactions via second-order consensus.

case, we reset the state to the initial value every 10 time units. A higher coefficient σ results in a higher tolerance in the synchronization dynamics. This is clear by looking at the plots from top to bottom in the left column.

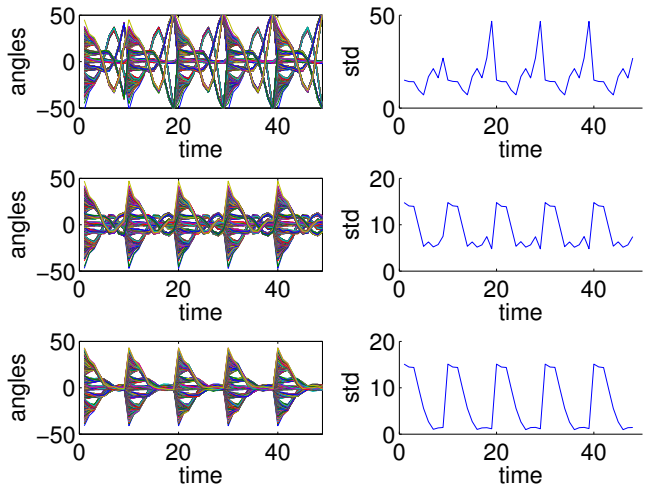

Figure 5: Inter-cluster oscillations: the influence of the damping coefficient in the second-order consensus. The plots display the time on the x-axis and the angles (left), and the standard deviation (right) on the y-axis.

7. Conclusions

This paper has studied synchronization via robust mean-field games. We have shown that in less prescriptive environments, where individuals' behaviors are not pre-programmed, synchronization may arise as an outcome of strategic thinking, prediction, and local interactions. We have also shown multi-scale phenomena involving fast local synchronization and slow inter-cluster oscillations. Future directions of research involve i) stability analysis under general topologies, ii) the extension of the framework to other coupling effects, and iii) the specialization of the model to electricity pricing.

Appendix

Proof of Theorem 1

To prove (14) let the Hamiltonian and robust Hamiltonian be:

$$H(x, \partial_x v_k(x,t), \rho_k) = \inf_u \left\{ \frac{1}{2} \left[a(\rho_k - x)^2 + cu^2 \right] + \partial_x v_k(x,t) u \right\} = 0,$$

$$\tilde{H}(x, \partial_x v_k(x,t), \overline{m}) = H(x, \partial_x v_k(x,t), \rho_k) + \sup_w \left\{ \partial_x v_k(x,t) w - \frac{1}{2}\gamma^2 w^2 \right\}.$$

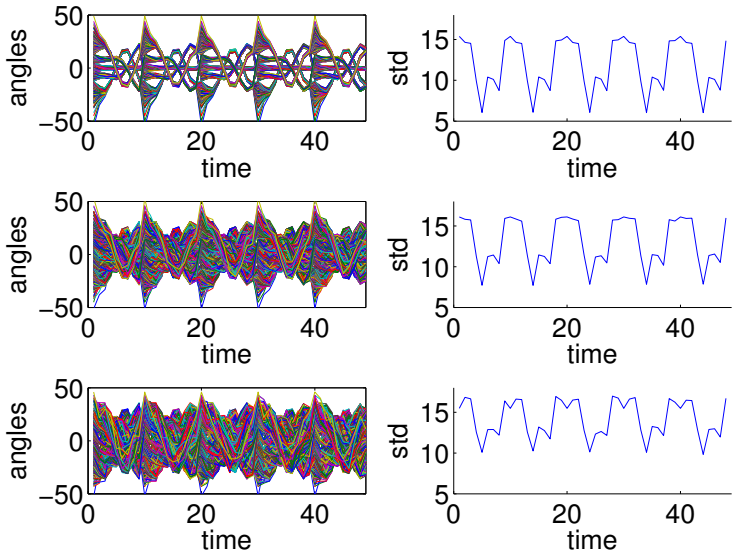

Figure 6: Inter-cluster oscillations: the influence of the Brownian motion coefficient σ. The plots display the time on the x-axis and the rotors' power angles (left), and the standard deviation (right) on the y-axis.

Differentiating with respect to u and w we obtain (14). To derive (13) note that the second and fourth equations are the boundary conditions and derive from the HJI equation and the evolution of the law of states.

To obtain the first equation, which is a PDE corresponding to the HJI, replace u_k^* appearing in the Hamiltonian (28) by its expression in (14):

$$H(x, \partial_x v_k(x,t), \rho_k) = \frac{1}{2}a(\rho_k - x)^2 - \frac{1}{2c}\Big(\partial_x v_k(x,t)\Big)^2.$$

Using the above expression of the Hamiltonian in the HJI equation in (12), we obtain the HJI in (13).

To obtain the third equation, which is a PDE representing the FPK equation, we simply plug (14) into the FPK in (12), and this concludes the proof.

Proof of Theorem 2

Isolating the HJI part of (13) for fixed ρ_k, we have

$$\begin{array}{l}\partial_t v_k(x,t) + \left(-\frac{1}{2c_1} + \frac{1}{2\gamma^2}\right)|\partial_x v_k(x,t)|^2 \\ +\frac{1}{2}a(\rho_k(t)-x)^2 + \frac{1}{2}\sigma^2\partial^2_{xx}v_k(x,t) = 0, \text{ in } \mathbb{R}\times[0,T[, \\ v_k(x,T) = \Psi(\rho_k(T),x), \text{ in } \mathbb{R}.\end{array} \tag{28}$$

Consider the value function

$$v_k(x,t) = \frac{1}{2}\phi(t)x^2 + h(t)x + \chi(t),$$

so that (28) can be rewritten as

$$\begin{array}{r}\frac{1}{2}\dot\phi(t)x^2 + \dot h(t)x + \dot\chi(t) + \left(-\frac{1}{2c_1} + \frac{1}{2\gamma^2}\right)[\phi(t)^2x^2 + h(t)^2 \\ +2\phi(t)h(t)x] + \frac{1}{2}a(\rho_k(t)^2 + x^2 - 2\rho_k(t)x) + \frac{1}{2}\sigma^2\phi(t) = 0 \text{ in } \mathbb{R}\times[0,T[, \\ \phi(T) = S, \quad h(T) = -S\rho_k(T), \quad \chi(T) = \frac{1}{2}S\rho_k(T)^2.\end{array}$$

Since this is an identity in x, it reduces to three equations:

$$\begin{array}{l}\dot\phi(t) + \left(-\frac{1}{c_1} + \frac{1}{\gamma^2}\right)\phi(t)^2 + a = 0 \text{ in } [0,T[, \ \ \phi(T) = S, \\ \dot h(t) + \left(-\frac{1}{2c_1} + \frac{1}{2\gamma^2}\right)2\phi(t)h(t) - a\rho_k(t) = 0 \\ \text{ in } [0,T[, \ h(T) = -S\rho_k(T), \\ \dot\chi(t) + \left(-\frac{1}{2c_1} + \frac{1}{2\gamma^2}\right)h(t)^2 + \frac{1}{2}a\rho_k(t)^2 \\ +\frac{1}{2}\sigma^2\phi(t) = 0 \text{ in } [0,T[, \ \chi(T) = \frac{1}{2}S\rho_k(T)^2.\end{array} \tag{29}$$

For the mean-field equilibrium control and worst-case disturbance we have

$$u^*(x,t) = -\tfrac{1}{c_1}(\phi(t)x + h(t)), \quad w^*(x,t) = \tfrac{1}{\gamma^2}(\phi(t)x + h(t)). \tag{30}$$

By averaging the above expressions and substituting in $\frac{d}{dt}\overline{m}_k(t) = \overline{u}_k(t) + \overline{w}_k(t)$ we obtain $\dot{\overline{m}}(t) = (-\frac{1}{c_1} + \frac{1}{\gamma^2})(\phi(t)\overline{m}_k(t) + h(t))$ as in (16). In the stationary case, i.e. $T\to\infty$, we obtain from (29)

$$\begin{array}{l}\left(-\frac{1}{c_1} + \frac{1}{\gamma^2}\right)\phi^2 + a = 0, \\ \left(-\frac{1}{c_1} + \frac{1}{\gamma^2}\right)\phi h - a\rho_k = 0, \\ \left(-\frac{1}{c_1} + \frac{1}{\gamma^2}\right)h^2 + a\rho_k^2 + \sigma^2\phi = 0.\end{array}$$

Solving for ϕ and h yields

$$h = \frac{1}{\phi\left(-\frac{1}{c_1}+\frac{1}{\gamma^2}\right)} a\rho_k = \frac{\phi}{\phi^2\left(-\frac{1}{c_1}+\frac{1}{\gamma^2}\right)} a\rho_k = -\phi\rho_k.$$

Substituting in (30), control and disturbance take the form

$$u^*(x,t) = \tfrac{1}{c_1}\phi(\rho_k - x), \quad w^*(x,t) = -\tfrac{1}{\gamma^2}(\rho_k - x).$$

Then, mean states of *neighbor* populations follow the *local interaction* rule

$$\begin{aligned}\tfrac{d}{dt}\overline{m}_k(t) &= \overline{u}_k(t) + \overline{w}_k(t) = \phi(\tfrac{1}{c_1} - \tfrac{1}{\gamma^2})(\tfrac{\sum_{j\in N(k)} \overline{m}_j(t)}{|N(k)|} - \overline{m}_k(t)) \\ &= \phi(\tfrac{1}{c_1} - \tfrac{1}{\gamma^2})\tfrac{1}{|N(k)|}(\textstyle\sum_{j\in N(k)}(\overline{m}_j(t) - \overline{m}_k(t))).\end{aligned}$$

In other words, local interaction involves a local averaging (the term including the Laplacian defined below) and a local adjustment. For the vector of aggregate states $\overline{m} = (\overline{m}_1, \overline{m}_2, \ldots, \overline{m}_p)^T$, we have the consensus dynamics $\dot{\overline{m}}(t) = -L\overline{m}(t)$, where L is the Laplacian matrix defined as

$$L_{kj} = \begin{cases} \phi(\frac{1}{c_1} - \frac{1}{\gamma^2}) & j = k, \\ -\phi(\frac{1}{c_1} - \frac{1}{\gamma^2})\frac{1}{|N(k)|} & j \in N(k),\ j \neq k, \\ 0 & \text{otherwise.} \end{cases}$$

Proof of Corollary 1

Since $G = (V, E)$ is a balanced graph (or undirected graph), we have that the second smallest eigenvalue $\lambda_2(\phi)$ is defined by

$$\min_{\mathbf{1}^T\xi} \frac{\xi^T L\xi}{\xi^T\xi} = \lambda_2(\phi).$$

The above implies that $\xi^T L\xi \geq \lambda_2(\phi)\|\xi\|^2$. Then

$$\dot{\nu}(\xi(t)) = -2\xi^T L\xi \leq -2\lambda_2(\phi)\xi^T\xi \leq -2\lambda_2(\phi)\nu(t).$$

Proof of Corollary 2

Let $X(t)$ be a solution of (24) with initial value $X(0) \notin \mathcal{X}$. Set $t = \{\inf t > 0 |\, X(t) \in \mathcal{X}\} \leq \infty$ and let $V(X(t)) = dist(X(t), \mathcal{X})$. For all $t \in [0, t]$

$$\begin{aligned}&V(X(t+dt)) - V(X(t)) = \|X(t) + dX(t) - \Pi_{\mathcal{X}}(X(t))\| - \|X(t) - \Pi_{\mathcal{X}}(X(t))\| \\ &= \tfrac{1}{\|X(t)+dX(t)-\Pi_{\mathcal{X}}(X(t))\|}\|X(t) + dX(t) - \Pi_{\mathcal{X}}(X(t))\|^2 \\ &-\tfrac{1}{\|X(t)-\Pi_{\mathcal{X}}(X(t))\|}\|X(t) - \Pi_{\mathcal{X}}(X(t))\|^2.\end{aligned}$$

From the definition of infinitesimal generator

$$\mathcal{L}V(X(t)) = \lim_{dt\to 0} \frac{\mathbb{E}V(X(t+dt)) - V(X(t))}{dt}$$
$$= \lim_{dt\to 0} \frac{1}{dt}\Big[\mathbb{E}\Big(\frac{1}{\|X(t)+dX(t)-\Pi_{\mathcal{X}}(X(t))\|}\|X(t)+dX(t)$$
$$-\Pi_{\mathcal{X}}(X(t))\|^2\Big) - \frac{1}{\|X(t)-\Pi_{\mathcal{X}}(X(t))\|}\|X(t)-\Pi_{\mathcal{X}}(X(t))\|^2\Big]$$
$$\leq \frac{1}{\|X(t)-\Pi_{\mathcal{X}}(X(t))\|}\Big[\partial_X V(X,t)^T\left(-\frac{1}{c_1}+\frac{1}{\gamma^2}\right)\Big(\phi(t)X(t)+h(t)\Big)\Big) + \frac{1}{2}\sigma^2\partial_{xx}V(X,t)\Big].$$

From (25) the above implies that $\mathcal{L}V(X(t)) < 0$, for all $X(t) \notin \mathcal{M}$.

Acknowledgments

The author would like to thank the anonymous reviewers for their valuable comments.

[1] D. Bauso, H. Tembine, T. Başar, Robust Mean Field Games, Dynamic Games and Applications, 6(3) (2016) 277–300.

[2] T.K. Dal'Maso Peron, F.A. Rodrigues, Collective behavior in financial markets, EPL (Europhysics Letters), 96(4) (2011).

[3] F. Dörfler, F. Bullo, Synchronization and Transient Stability in Power Networks and Nonuniform Kuramoto Oscillators, SIAM Journal on Control Optimization, 50(3) (2012) 1616–1642.

[4] D.A. Gomes, J. Saúde, Mean Field Games Models - A Brief Survey, Dynamic Games and Applications, 4(2) (2014) 110–154.

[5] High-frequency trading synchronizes prices in financial markets, Said Business Sc., Oxford, http://www.www.sbs.ox.ac.uk/faculty-research/insights-research/finance/high-frequency-trading-synchronizes-prices-financial-markets (accessed 30.08.16).

[6] M.Y. Huang, P.E. Caines, R.P. Malhamé, Individual and Mass Behaviour in Large Population Stochastic Wireless Power Control Problems: Centralized and Nash Equilibrium Solutions, IEEE Conference on Decision and Control, HI, USA, December, pp. 98–103, 2003.

[7] M.Y. Huang, P.E. Caines, R.P. Malhamé, Large Population Stochastic Dynamic Games: Closed Loop Kean-Vlasov Systems and the Nash Certainty Equivalence Principle, Communications in Information and Systems, 6(3) (2006) 221–252.

[8] M.Y. Huang, P.E. Caines, R.P. Malhamé, Large population cost-coupled LQG problems with non-uniform agents: individual-mass behaviour and decentralized ϵ-Nash equilibria, IEEE Transactions on Automatic Control, 52(9) (2007) 1560–1571.

[9] P. Jia, P.E. Caines, Analysis of Decentralized Quantized Auctions on Cooperative Networks, IEEE Transactions on Automatic Control, 52(2) (2013) 529–534.

[10] J.-M. Lasry, P.-L. Lions, Mean field games, Japanese Journal of Mathematics, 2 (2007) 229–260.

[11] K. A. Loparo, X. Feng, Stability of stochastic systems, The Control Handbook, CRC Press, (1996) 1105–1126.

[12] R. Olfati-Saber, J.A. Fax, R.M. Murray, Consensus and Cooperation in Networked Multi-Agent Systems, Proc. of IEEE, 95(1) (2007) 215–233.

[13] A. Pluchino, V. Latora, and A. Rapisarda, Compromise and synchronization in opinion dynamics, The European Physical Journal B - Condensed Matter and Complex Systems, 50(1-2) (2006) 169–176.

[14] H. Tembine, Q. Zhu, T. Başar, Risk-sensitive mean-field games, IEEE Transactions on Automatic Control, 59(4) (2014) 835–850.

[15] H. Yin, P. G. Mehta, S. P. Meyn, U. V. Shanbhag, Synchronization of Coupled Oscillators is a Game, IEEE Transactions on Automatic Control, 57(4) (2012) 920–935.

[16] H. Yin, P. G. Mehta, S. P. Meyn, U. V. Shanbhag, Learning in Mean-Field Games, IEEE Trans. on Automatic Control, 59(3) (2014) 629–644.

[17] H. Yin, P. G. Mehta, S. P. Meyn, U. V. Shanbhag, On the Efficiency of Equilibria in Mean-Field Oscillator Games, Dynamic Games and Applications, 4(2) (2014) 177–207.